

Electromyogram Amplitude Estimation with Adaptive Smoothing Window Length

Edward A. Clancy, *Senior Member, IEEE*

Abstract—Typical electromyogram (EMG) amplitude estimators use a fixed window length for smoothing the amplitude estimate. When the EMG amplitude is dynamic, previous research suggests that varying the smoothing length as a function of time may improve amplitude estimation. This paper develops optimal time-varying selection of the smoothing window length using a stochastic model of the EMG signal. Optimal selection is a function of the EMG amplitude and its derivatives. Simulation studies, in which EMG amplitude was changed randomly, found that the “best” adaptive filter performed as well as the “best” fixed-length filter. Experimental studies found the advantages of the adaptive processor to be situation dependent. Subjects used real-time EMG amplitude estimates to track a randomly-moving target. Perhaps due to task difficulty, no differences in adaptive versus fixed-length processors were observed when the target speed was fast. When the target speed was slow, the experimental results were consistent with the simulation predictions. When the target moved between two constant levels, the adaptive processor responded rapidly to the target level transitions and had low variance while the target dwelled on a level.

Index Terms—Biomedical signal processing, biological system modeling, electromyogram (EMG) amplitude estimation, electromyography, modeling, myoelectric signal processing.

I. INTRODUCTION

THE amplitude of the surface EMG is frequently used to control myoelectric prostheses, as a measure of muscular effort, and as an indicator of muscle force. Early investigators of EMG amplitude estimation methods studied the type of nonlinear detector which should be applied to the signal [1]–[5]. This work led to analog-rectify-and-smooth processing or root-mean-square (RMS) processing as the standard techniques for EMG amplitude estimation. Whitening individual EMG signal channels [1], [2], [6]–[10], and combining multiple signal channels into a single EMG amplitude estimate [1], [2], [9], [11]–[13] have been shown to provide a higher fidelity EMG amplitude estimator.

When muscle contraction is dynamic, i.e., when either the exerted force, or muscle length, or both change during the contraction, selection of an appropriate smoothing window length has been a topic of study. It is important to study this condition since most muscle contraction is dynamic. In this case, variance (random) errors in the EMG amplitude estimate are diminished with a long smoothing window; however, bias (deterministic) errors in tracking the signal of interest are

diminished with a short smoothing window. For fixed-length smoothers, an appropriate balance needs to be established. Inman *et al.* [3] (this work is generally attributed to be the first continuous EMG amplitude estimator) approached this problem by evaluating three different time constants for their analog RC low-pass filter. They qualitatively selected the best time constant for their application. Hershler and Milner [14] developed an optimality criterion for quantitative empirical evaluation of optimal window length for use in human locomotion studies. They found that the optimal window length varied with the walking speed. A model-based approach to selecting the best time constant was taken by Miyano *et al.* [15] in developing a procedure to obtain the optimal time constant for a full-wave rectified detector. They showed that the optimal time constant could be determined by minimizing a nonlinear equation related to the autocorrelation coefficient function of muscle contraction level. Xiong and Shweddyk [16] described a stochastic model of the EMG and found that a noncausal (i.e., midpoint moving average) smoothing window worked best for nonstationary EMG amplitude estimates. Selection of the optimum window size depended on the characteristics of the EMG amplitude. They studied ramp, trapezoidal and sinusoidal changes in EMG amplitude. In general, numerical methods were required to determine the optimum window length. An analytic solution was available if the EMG amplitude changed in a ramp fashion.

Rather than find one fixed-length window size which is optimal for an entire application, a better EMG amplitude estimate may be achieved if the smoothing window length is adapted to the local characteristics of the amplitude signal. In general, when the amplitude is changing rapidly, the window length should be short; when the amplitude is changing slowly, the window length should be long. Jerard *et al.* [17] implemented a simple adaptive window length estimator, via a nonlinear analog circuit, into the EMG control of the Liberty Mutual Boston Elbow. D’Alessio [7], [18] argued that, theoretically, dynamic tuning of the window length should be a function of the EMG amplitude and its first two derivatives. However, since estimation of the second derivative seemed too difficult, D’Alessio implemented a technique based on the EMG amplitude and its first derivative. The technique was evaluated on simulated EMG signals. Meek and Fetherston [19] and Park and Meek [20] (see also [21] and [22]) described adaptive techniques also based on the EMG amplitude and its first derivative. Their work quantitatively evaluated processor performance. When contraction level was rapidly changing or slowly changing, the adaptive processors

Manuscript received April 8, 1998; revised November 3, 1998.

The author is with the Liberty Mutual Research Center for Safety and Health, 71 Frankland Road, Hopkinton, MA 01748 USA (e-mail: ted.clancy@alum.wpi.edu).

Publisher Item Identifier S 0018-9294(99)03987-7.

provided an improvement over certain fixed-length smoothing window processors. Their work has been incorporated into the EMG control scheme of the Utah arm [23]. As an alternative to these methods, Evans *et al.* [24] proposed an amplitude estimation scheme using a multiplicative (signal multiplied by noise) mathematical model of EMG. Evans *et al.* proposed a logarithmic transformation of the myoelectric signal. This transformation yields an additive (signal plus noise) representation of the EMG. They then applied the theory of Kalman filters to estimate the amplitude of the transformed signal.

Taken together, these results suggest a role for adaptive window length processing in EMG amplitude estimation. These techniques could be used to reduce the error in EMG amplitude estimates used in applications such as prosthetic control, analysis of gait, motion control studies, etc. However, the techniques for adaptive smoothing window length processors are not completely developed, and the relative merits of each proposed technique are not known. A method for selecting an appropriate technique for a given application—or perhaps identifying a globally “optimal” technique—is not available. Optimal and user independent techniques could also lead to increased standardization of EMG amplitude estimation techniques among different labs. Further, quantitative characterization of the improvement due to adaptive smoothing is needed over a wider range of EMG applications as well as a wider range of EMG processing schemes.

This report describes the design and characterization of an adaptive window length processor. First, an adaptive window length processor is mathematically derived. This model utilizes theoretical and experimental results from previous studies of stationary EMG processing, with extensions relevant to dynamic amplitude estimation. The model considers both the causal and noncausal processing situations. Second, the new technique is studied using a stochastic simulation model of the EMG signal. The simulation evaluates the expected performance of the adaptive algorithms. Third, an experimental evaluation of the technique is described. Constant-angle, force-varying (dynamic), nonfatiguing contractions were studied while subjects performed a real-time tracking task. A preliminary report of this work has appeared in [25].

II. DEVELOPMENT OF THE ADAPTIVE ESTIMATOR

The mean square error (MSE) in the EMG amplitude estimate can be written as the sum of two components: a variance component $\sigma^2(t)$ (due to random fluctuations in the EMG amplitude estimate about the true amplitude) and a bias component $b(t)$ (due to errors in tracking true changes in the amplitude) [7], [18], [20]

$$\text{MSE}(t) = \sigma^2(t) + b^2(t) \quad (1)$$

where t is the discrete sample index. Writing the MSE in this fashion allows each component to be evaluated separately. In general, variance error is reduced with a large duration smoothing window and bias error is reduced with a small duration smoothing window. For improved amplitude estimation (i.e., minimum MSE), therefore, the smoothing window length should be dynamically tuned to the characteristics of the EMG

amplitude each instant in time. To do so, bias and variance will each be written as a function of the smoothing window length, and then the MSE minimized.

A. Variance Component of the Error

For the variance component, define the signal to noise ratio (SNR) of EMG amplitude estimates from a constant-angle, constant-force, nonfatiguing contraction trial as the mean value of the amplitude estimate $\hat{s}(t)$ divided by its standard deviation. Assume the standard functional¹ stochastic model [1], [6]–[8], [11], [18] in which the EMG *signal* is considered as a zero-mean, band-limited, wide sense stationary, correlation-ergodic, random process multiplied by the EMG *amplitude*. The EMG signal is frequently considered to be Gaussian distributed. For these conditions, Hogan and Mann [1], [2] and St-Amant *et al.* [26] showed that the SNR is closely approximated as

$$\text{SNR} = \sqrt{\frac{2 \cdot N \cdot g(B_s, L, D)}{f}}$$

where N is the window length in samples, f is the sampling frequency (in Hertz) and g is a constant determined by B_s , L and D . B_s is the *statistical bandwidth* (related to the equivalent number of independent samples in a signal [27]) of the EMG data (in Hertz). L is the number of EMG channels which are combined to form the amplitude estimate. (Each channel is assumed to have the same statistical bandwidth.) D denotes the detector type—either mean-absolute-value (MAV) or RMS. (For example, using RMS processing and assuming the standard Gaussian model for the EMG, then $g = 2B_s \cdot L$.) For these conditions, the mean value of the amplitude estimate is equal to the true amplitude value $s(t)$, permitting the SNR to be written as $\text{SNR} = s(t)/\sigma(t)$. Thus

$$\sigma^2(t) = \frac{f \cdot s^2(t)}{2 \cdot N \cdot g(B_s, L, D)}. \quad (2)$$

This variance changes, with respect to N , as $d\sigma^2(t)/dN = (-f \cdot s^2(t))/(2 \cdot N^2 \cdot g(B_s, L, D))$.

B. Bias Component of the Error

For the bias component, consider the error that occurs if no variance error exists (i.e., the EMG *signal* consists only of the EMG *amplitude*), but the EMG amplitude is dynamically changing. In particular, let the EMG amplitude in the neighborhood of sample t be modeled as the quadratic polynomial

$$s(t) = a_0 + a_1 t + a_2 t^2 \quad (3)$$

where a_0 , a_1 and a_2 are constants, and t is the discrete sample index. A polynomial model was selected for its simplicity. As will be shown subsequently, each polynomial degree requires the computation of an additional derivative of EMG amplitude. Prior research [7] suggests that derivatives of EMG

¹The term “functional” signifies that the model is based on the observed signal phenomenon, as opposed to a model which describes the underlying physiological process.

amplitude are quite noisy, particularly as the derivative order increases. Thus, the polynomial model was limited to second degree (corresponding to first and second derivatives of EMG amplitude). With this model, the amplitude value at sample $t - k$, is

$$s(t - k) = s(t) - \frac{k\dot{s}(t)}{f} + \frac{k^2}{2f^2}\ddot{s}(t) \quad (4)$$

where $\dot{s}(t) = a_1f + 2a_2ft$ is the derivative of $s(t)$ with respect to time (expressed in units of EMG amplitude per second [28]) and $\ddot{s}(t) = 2a_2f^2$ is the second derivative with respect to time. If an MAV detector is used to form the amplitude estimate \hat{s} at sample t from N EMG signal samples, then

$$\hat{s}(t) = \frac{1}{N} \sum_{i=0}^{N-1} |m(t+h-i)| \quad (5)$$

where $m(t)$ are the EMG signal samples and h is an integer offset which controls the causality of the estimator. Setting h to zero gives a causal estimator. Setting h to $(N-1)/2$, for N odd, gives a noncausal window centered at sample t . However, since the bias is the error that occurs if the stochastic portion of the EMG signal is removed, the EMG signal $m(t+h-i)$ in (5) can be replaced by the true EMG amplitude $s(t+h-i)$ (which is always nonnegative), to give

$$\hat{s}(t) = \frac{1}{N} \sum_{i=0}^{N-1} [s(t+h-i)]. \quad (6)$$

Substituting the relation in (4) into (6) and simplifying gives

$$\hat{s}(t) = \frac{1}{N} \left[Ns(t) + \frac{Nh}{f}\dot{s}(t) - \frac{\dot{s}(t)}{f} \sum_{i=0}^{N-1} i + \frac{Nh^2}{2f^2}\ddot{s}(t) - \frac{h\dot{s}(t)}{f^2} \sum_{i=0}^{N-1} i + \frac{\ddot{s}(t)}{2f^2} \sum_{i=0}^{N-1} i^2 \right].$$

The remaining three sums can be simplified [29] to give

$$b(t) = \frac{h}{f}\dot{s}(t) - \frac{\dot{s}(t)}{2f}(N-1) + \frac{h^2}{2f^2}\ddot{s}(t) - \frac{h}{2f^2}\dot{s}(t)(N-1) + \frac{\ddot{s}(t)}{12f^2}(2N^2 - 3N + 1)$$

where the bias error has been defined as $b(t) = \hat{s}(t) - s(t)$.

C. MSE—Causal Processing

For the causal case (i.e., $h = 0$), the bias becomes

$$b(t)|_{h=0} = \frac{(N-1)}{2f} \left[\frac{\dot{s}(t)(2N-1)}{6f} - \dot{s}(t) \right].$$

If $\text{MSE}(t)$ is now written, the optimal window length can theoretically be found by differentiating with respect to N , setting the derivative to zero, and then solving for N . Unfortunately, this approach leads to a complex nonlinear equation. Hence,

an exhaustive numerical search was used instead. To find an optimum N , $\text{MSE}(t)$ was computed for all possible window lengths corresponding to a duration ranging from 50–1000 ms, and the length corresponding to the minimum error was selected.

D. MSE—Noncausal Processing

For a noncausal window centered on sample t [i.e., $h = (N-1)/2$] the bias becomes

$$b(t)|_{h=(N-1)/2} = \frac{\dot{s}(t)(N^2-1)}{24f^2}. \quad (7)$$

Squaring this bias and differentiating with respect to N gives

$$\begin{aligned} \left. \frac{db^2(t)}{dN} \right|_{h=(N+1)/2} &= \frac{\dot{s}^2(t)}{576f^4} \cdot 2(N^2-1) \cdot 2N \\ &= \frac{\dot{s}^2(t)}{144f^4} (N^2-1)N. \end{aligned}$$

The derivative of MSE [see (1)], with respect to N , then becomes

$$\begin{aligned} \left. \frac{d\text{MSE}(t)}{dN} \right|_{h=(N+1)/2} &= \frac{\dot{s}^2(t)}{144f^4} (N^2-1)N \\ &\quad - \frac{fs^2(t)}{2N^2g(B_s, L, D)}. \end{aligned}$$

Setting this derivative to zero and solving for N provides the optimum value for N . To do so, the following polynomial in N must be solved:

$$N^5 - N^3 = \frac{72f^5s^2(t)}{g(B_s, L, D)\dot{s}^2(t)}.$$

If N is not small, $N^5 - N^3 \cong N^5$ (for $N > 10$, the error in this approximation is less than 1% of the true value), giving

$$\frac{N(t)_{\text{noncausal, quadratic}}}{f} \cong \left[\frac{72}{g(B_s, L, D)} \right]^{1/5} \cdot \left[\frac{s^2(t)}{\dot{s}^2(t)} \right]^{1/5}. \quad (8)$$

Fig. 1 plots this result.

E. Linear Model of EMG Amplitude Variation

Because (3) models the EMG amplitude in the neighborhood of sample t as a quadratic polynomial, adaptive estimators with second derivative terms result [see (8)]. In practice, limiting the solution to first derivative terms may be required since computation of second derivatives may be too noisy [7]. This restriction can be accomplished by using a linear model of EMG amplitude in the neighborhood of sample t , i.e., by setting $\ddot{s}(t) = 0$ in (4). For causal processing, this linear model gives a $d\text{MSE}(t)/dN$ of

$$\begin{aligned} \left. \frac{d\text{MSE}(t)}{dN} \right|_{h=0, \text{ linear}} &= \frac{N\dot{s}^2(t)}{2f^2} - \frac{\dot{s}^2(t)}{2f^2} \\ &\quad - \frac{f \cdot s^2(t)}{2 \cdot N^2 \cdot g(B_s, L, D)}. \end{aligned}$$

Setting this derivative to zero and solving for N gives

$$N^3 - N^2 = \frac{f^3}{g(B_s, L, D)} \cdot \frac{s^2(t)}{\dot{s}^2(t)}.$$

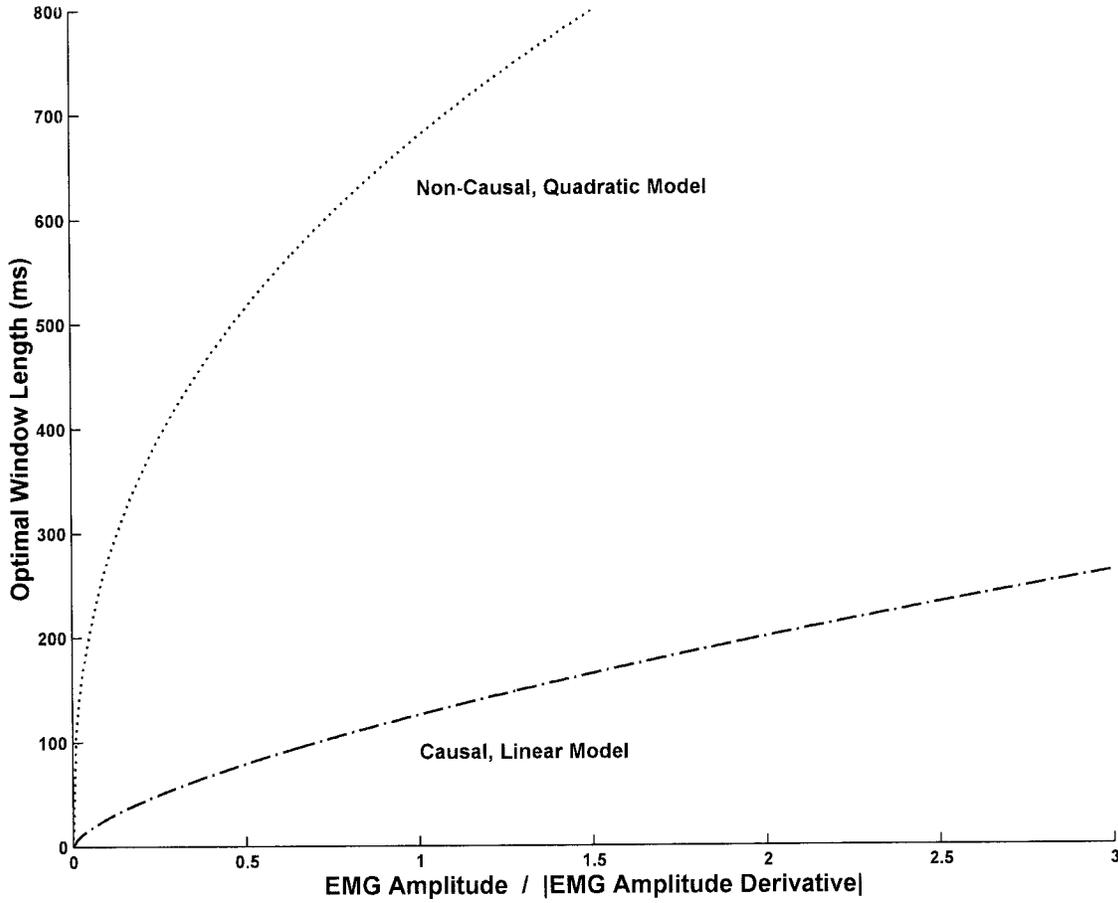


Fig. 1. Theoretical optimal smoothing window lengths. Dotted graph is for the noncausal quadratic model described by (8). For this plot, the X -axis is the ratio of EMG amplitude to EMG amplitude second derivative magnitude (in units of seconds squared). Dot-dash graph is for the causal linear model described by (9). For this plot, the X -axis is the ratio of EMG amplitude to EMG amplitude first derivative magnitude (in units of seconds). For both graphs, the constant g is set to 500/s.

For N large, $N^3 - N^2 \cong N^3$, (for $N > 100$, the error in this approximation is less than 1% of the true value), giving

$$\frac{N(t)_{\text{causal, linear}}}{f} \cong \frac{1}{g^{1/3}(B_s, L, D)} \cdot \left[\frac{s^2(t)}{\dot{s}^2(t)} \right]^{1/3}. \quad (9)$$

Fig. 1 plots this result.

For noncausal processing (window centered at sample t), the bias error with this model is zero [substitute $\ddot{s}(t) = 0$ into (7)]. In other words, this model fails to capture any bias error component. Hence, no adaptive estimator results from this formulation. To coerce a solution, the above causal linear result for the optimum window selection (9) was used, combined with noncausal estimation of the EMG amplitude and its derivative.

III. SIMULATION STUDY

A. Two-Pass Adaptive Window Technique

Implementation of any of these adaptive processors presupposes the true value of the EMG amplitude and its derivatives. In practice, these values are not known and must be estimated from the EMG signal. Hence, the adaptive algorithm was implemented in two passes. In the first pass, fixed-length

processing stages were used to estimate the EMG amplitude and its derivatives. Derivatives were estimated by numerically differentiating the rectified EMG signal, as detailed below. The adaptive window length N was then selected for each sample index. For causal processing, the optimum N is rounded to the nearest integer value, for noncausal centered window processing, the optimum N is rounded to the nearest odd integer value. In the second pass, the adaptive N was implemented to produce the adaptive amplitude estimate. Simulation was used to investigate the effectiveness of this two-pass method.

B. Simulation Methods

Initially, the expected performance of the adaptive window length algorithm versus fixed length algorithms was investigated. Each condition was investigated with one simulation, 196 s in duration. (Two additional initial and final seconds of simulation data were discarded so as to avoid transients at the end points.) In an actual experimental situation, the window length would be constrained to a minimum and maximum value so that it would not fluctuate without bound. Thus, in this simulation work, the minimum and maximum window durations were set to 50 and 1000 ms, respectively. Adaptive estimators were evaluated twice: first, with the derivatives

TABLE I
PREFERRED POLYNOMIAL FILTER SMOOTHING LENGTH (IN SECONDS) FOR EMG AMPLITUDE DERIVATIVE ESTIMATION. RESULTS ARE GIVEN FOR FIRST AND SECOND DERIVATIVES USING CAUSAL AND NONCAUSAL FILTERS. “—” DENOTES THAT NO PREFERRED LENGTH WAS FOUND

Estimated Derivative	Tracking Bandwidth					
	0.1 Hz	0.25 Hz	0.5 Hz	1 Hz	2 Hz	4 Hz
First Derivative; Causal	1.625	1.125	0.5	0.375	0.25	—
First Derivative; Non-Causal	3.5	2	1	0.5	0.25	0.125
Second Derivative; Causal	2	1.875	1.25	0.625	—	—
Second Derivative; Non-Causal	4	2.5	1.25	0.75	0.5	0.25

known (to establish “ideal” technique performance) and second, with the derivatives estimated from the EMG signal (as would be done with actual data). Evaluation consisted of computing the mean absolute error between the simulated EMG *amplitude* and that estimated from the simulated EMG *signal*. The preferred length polynomial differentiator was used for each target bandwidth.

Next, the rate at which adaptation was allowed to take place was studied to determine its influence on adaptive processor performance. In all of the previous simulation conditions, no bound was placed on the sample-to-sample change in the window length (except that the duration remained within 50–1000 ms). In practice, however, it is common to limit the rate of adaptation in order to achieve a more stable adaptive process. Limiting the rate of change is also consistent with the limits by which the physiology allows EMG amplitude (and its derivatives) to change. To limit the rate of change, each new optimum window length was successively compared to the immediate past window length. If the new window length changed more than the limit amount, the new window length was set to the value corresponding to the maximum change. This nonlinear scheme was performed on the optimum window lengths prior to rounding them off to integer values; thus, the limit value could be less than the duration of one sample period. Using this scheme, the adaptive window length simulations were rerun (the first-pass smoothing window length was fixed as 250 ms) with the change in the window length limited to various values over the range of 0.01–100 ms per iteration.

For each simulation, the EMG *signal* was simulated by passing uncorrelated, unit-variance, Laplacian random noise through a low-pass filter (256 Hz) and then multiplying this signal by the simulated EMG *amplitude*. The filtered Laplacian process provided an EMG signal whose density was more peaked than a Gaussian process, consistent with experimental observations [30], [31]. EMG *amplitude* was designed to change as a band-limited random process with uniform density ranging from simulated relaxation to simulated 50% maximum voluntary EMG (MVE). (MVE refers to the EMG amplitude level corresponding to MVC, or “maximum voluntary contraction.” This level is determined from a constant-angle, constant-force, nonfatiguing contraction and therefore should not be a function of the EMG amplitude processing technique.) The simulated EMG amplitude was numerically differentiated

twice, to provide reference first- and second-derivative signals. Derivative estimates, derived from the simulated EMG signal were compared to these reference signals. All simulations were performed using MATLAB (version 5.2, The MathWorks, Natick, MA) on an IBM-compatible PC, using a simulated sampling frequency of 1024 Hz. The constant g was set to 500/s (see [26, Table II]), roughly corresponding to the appropriate value for the four-channel, MAV processor used in the experimental work.

During initial investigation with the model, smoothed differencing filters were used to estimate EMG *amplitude* derivatives from the EMG *signal*. Comparison of these estimated derivatives to the reference derivatives quickly showed these estimates to be inadequate. Thus, polynomial derivative filters (also known as Savitsky–Golay smoothing filters [28]) of degrees 1–5 were investigated. These filters were designed using software described in [28] and then loaded into MATLAB. Simulated EMG amplitude sequences with statistical bandwidths of 0.1, 0.25, 0.5, 1, 2 and 4 Hz were evaluated. The number of samples used in the polynomial filter was varied over a range representing 15.6 ms–2 s for causal filtering and 31.3 ms–4 s for noncausal filtering. Each condition was investigated by averaging the results from 40 simulations, each 20 s in duration.

C. Simulation Results

For the derivative filters, lower errors were consistently found using noncausal (centered window) filters as compared to causal filters. All errors grew as the tracking bandwidth increased. For noncausal filters, polynomial degree had little or no influence on derivative errors. For causal filters, a degree one polynomial was best for the first derivative and a degree two polynomial was best for the second derivative. Hence, all further description of results refers to these polynomial degrees. It was also found that the number of samples over which the polynomial filter should be fit varied with the target bandwidth. Table I lists the duration of the polynomial smoothing filter which gave the best performance for the various target bandwidths and derivatives. Note that second derivatives require a longer polynomial smoothing filter duration than first derivatives, consistent with the results of Giakas and Baltzopoulos [32]. Table II gives the mean absolute value errors using the best filter durations for causal/noncausal first/second derivative filters. Table II also lists the “default

TABLE II

MAV ERRORS IN EMG AMPLITUDE DERIVATIVE ESTIMATES. DERIVATIVES WERE ESTIMATED USING POLYNOMIAL FILTERS. DEFAULT ERROR IS THE ERROR THAT WOULD OCCUR IF THE DERIVATIVE VALUE AT ALL TIMES IS SET TO THE MEAN VALUE OF THE DERIVATIVE. FIRST DERIVATIVE ERRORS IN UNITS OF NORMALIZED EMG AMPLITUDE/S, SECOND DERIVATIVE ERRORS IN UNITS OF NORMALIZED EMG AMPLITUDE/S²

Target Bandwidth (Hz)	First Derivatives			Second Derivatives		
	Causal Filter Error	Non-Causal Filter Error	Default Error	Causal Filter Error	Non-Causal Filter Error	Default Error
0.1	0.022	0.007	0.048	0.045	0.010	0.029
0.25	0.068	0.022	0.123	0.146	0.055	0.169
0.5	0.154	0.051	0.242	0.625	0.258	0.672
1	0.365	0.129	0.473	2.661	1.112	2.705
2	0.852	0.307	0.933	≈10	5.100	10.715
4	1.800	0.808	1.877	≈32	21.823	42.624

TABLE III

MAV SIMULATION ERRORS (IN PERCENT MVE) FOR CAUSAL PROCESSING. RESULTS ARE GIVEN FOR ADAPTIVE (TOP) AND FIXED (BOTTOM) LENGTH PROCESSING. "—" DENOTES THAT THE SIMULATION WAS NOT EVALUATED SINCE NO USABLE DERIVATIVE ALGORITHM EXISTED FOR THE CONDITION. BOLDED CELLS DENOTE THE OPTIMUM FIXED-LENGTH PROCESSOR FOR EACH RESPECTIVE BANDWIDTH

CAUSAL PROCESSING						
Smoothing Window	Tracking Bandwidth					
	.1 Hz	.25 Hz	.5 Hz	1 Hz	2 Hz	4 Hz
Adaptive, Linear, Derivative Known	1.22	1.74	2.85	3.58	4.66	6.53
Adaptive, Quadratic, Derivative Known	1.23	1.62	2.46	3.02	3.90	5.43
Adaptive, Linear, Derivative Estimated	1.36	1.95	2.76	3.68	4.35	—
Adaptive, Quadratic, Derivative Estimated	1.66	2.19	3.31	6.07	—	—
Fixed, 50 ms	3.45	3.37	4.19	4.00	4.42	5.71
100 ms	2.47	2.47	3.19	3.39	4.61	7.57
150 ms	2.02	2.15	2.92	3.66	5.67	9.65
200 ms	1.77	2.02	2.97	4.21	6.84	10.93
250 ms	1.63	2.01	3.17	4.86	7.94	11.44
300 ms	1.53	2.06	3.44	5.54	8.89	11.52
350 ms	1.46	2.16	3.76	6.23	9.65	11.48
400 ms	1.42	2.29	4.12	6.91	10.22	11.47
450 ms	1.41	2.44	4.48	7.54	10.61	11.51
500 ms	1.40	2.59	4.85	8.14	10.85	11.56
550 ms	1.42	2.76	5.22	8.68	10.98	11.59
600 ms	1.45	2.93	5.59	9.18	11.04	11.63
650 ms	1.48	3.11	5.96	9.64	11.06	11.67
700 ms	1.52	3.30	6.32	10.02	11.08	11.71
750 ms	1.57	3.48	6.68	10.36	11.11	11.72
800 ms	1.62	3.67	7.02	10.64	11.14	11.72
850 ms	1.68	3.86	7.35	10.88	11.17	11.73
900 ms	1.74	4.06	7.68	11.07	11.19	11.75
950 ms	1.80	4.24	7.99	11.21	11.23	11.77
1000 ms	1.86	4.43	8.29	11.33	11.27	11.78

error," which is the error that would occur if the derivative value is always arbitrarily assigned its mean value over the entire sequence. This mean value was indistinguishable from zero for each of these simulations. Note that certain causal derivative filtering conditions at high bandwidths produced errors near the default error level (Table II) and had no identifiable optimum filter length (Table I).

Tables III and IV give the results for the adaptive window length algorithm versus fixed length algorithms simulations. Note that the adaptive window length processors were not sensitive to the method of estimating the first-pass EMG amplitude; hence, results are listed with a 250 ms smoothing window used on the first pass. The results show that for causal processing, the first derivative adaptive algorithm performs better than the second derivative technique (compare rows three and four in Table III). For each target bandwidth,

the adaptive algorithm (with estimated derivatives) performs about as well as the *best* fixed-length algorithm and better than all other fixed-length algorithms. For noncausal (centered window) processing, the second derivative adaptive algorithm performed better than the first derivative technique (compare rows three and four in Table IV). This performance level was again similar to the best fixed window length processor and better than all other fixed-length algorithms. Finally, when studying the adaptation rate, results for all bandwidths showed that the error in the EMG amplitude estimate was not influenced by the limit adaptation rate value.

IV. EXPERIMENTAL STUDY

The knowledge developed from these simulations was next used to guide an experimental evaluation of the causal adaptive estimator. Constant-angle, force-varying (dynamic),

TABLE IV
MAV SIMULATION ERRORS (IN PERCENT MVE) FOR *NONCAUSAL* PROCESSING. RESULTS ARE GIVEN FOR ADAPTIVE (TOP) AND FIXED (BOTTOM) LENGTH PROCESSING. BOLD FACES DENOTE THE OPTIMUM FIXED-LENGTH PROCESSOR FOR EACH RESPECTIVE BANDWIDTH

NON-CAUSAL PROCESSING						
Smoothing Window	Tracking Bandwidth					
	.1 Hz	.25 Hz	.5 Hz	1 Hz	2 Hz	4 Hz
Adaptive, Linear, Derivative Known	1.11	1.40	2.13	2.56	3.41	4.10
Adaptive, Quadratic, Derivative Known	0.79	0.88	1.26	1.58	2.18	2.96
Adaptive, Linear, Derivative Estimated	1.45	1.62	2.10	2.52	3.26	4.12
Adaptive, Quadratic, Derivative Estimated	0.83	0.96	1.27	1.69	2.37	3.29
Fixed, 50 ms	3.45	3.35	4.14	3.87	3.97	4.13
100 ms	2.45	2.39	2.95	2.74	2.87	3.29
150 ms	2.00	1.97	2.39	2.27	2.50	3.67
200 ms	1.74	1.71	2.07	2.02	2.48	4.67
250 ms	1.56	1.51	1.85	1.89	2.70	5.98
300 ms	1.43	1.38	1.70	1.86	3.07	7.22
350 ms	1.32	1.28	1.60	1.89	3.59	8.32
400 ms	1.23	1.20	1.53	1.99	4.19	9.16
450 ms	1.16	1.14	1.49	2.13	4.81	9.73
500 ms	1.10	1.09	1.47	2.32	5.47	10.11
550 ms	1.05	1.06	1.47	2.55	6.08	10.34
600 ms	1.00	1.03	1.48	2.82	6.68	10.48
650 ms	0.96	1.00	1.52	3.12	7.24	10.57
700 ms	0.93	0.99	1.57	3.42	7.71	10.63
750 ms	0.90	0.97	1.64	3.76	8.14	10.69
800 ms	0.87	0.96	1.71	4.09	8.50	10.75
850 ms	0.85	0.96	1.81	4.43	8.81	10.82
900 ms	0.83	0.96	1.91	4.78	9.06	10.88
950 ms	0.81	0.96	2.03	5.12	9.27	10.94
1000 ms	0.79	0.97	2.15	5.46	9.43	10.99

nonfatiguing contractions were studied in a tracking task. Only the first derivative adaptive processor was implemented since it gave results superior to the second derivative adaptive processor in the simulations.

A. Experimental Apparatus

Fig. 2 is a photograph of the experimental apparatus. A subject was seated in the firmly cushioned seat of a Biodex exercise machine (Biodex Medical Systems, Inc., Shirley, NY) and secured to the seat back rest via three quick release belts. The subject's right arm was oriented so that the upper arm and forearm were in the plane parallel to the floor (shoulder abducted 90° from the anatomic position), the forearm was oriented in the parasagittal plane, with the wrist in complete supination, and the angle between the upper arm and the forearm was 90° . The subject's right wrist, at the level of the styloid process was fit into a cuff which was rigidly attached to the dynamometer of the Biodex. The position and orientation of the dynamometer was fixed throughout the experiment. The dynamometer provided a measure of constant-angle torque generated about the elbow.

Prior to electrode placement, the skin above the investigated muscles was cleaned with an alcohol wipe and a small amount of electrode paste was applied. For each of the biceps (flexor) and triceps (extensor) muscles, an array of four EMG electrode-amplifiers (Liberty Technology model MYO115, Hopkinton, MA) was placed in-line, side-by-side, transversely across the muscle, located approximately midway between the elbow and the midpoint of the upper arm, clus-

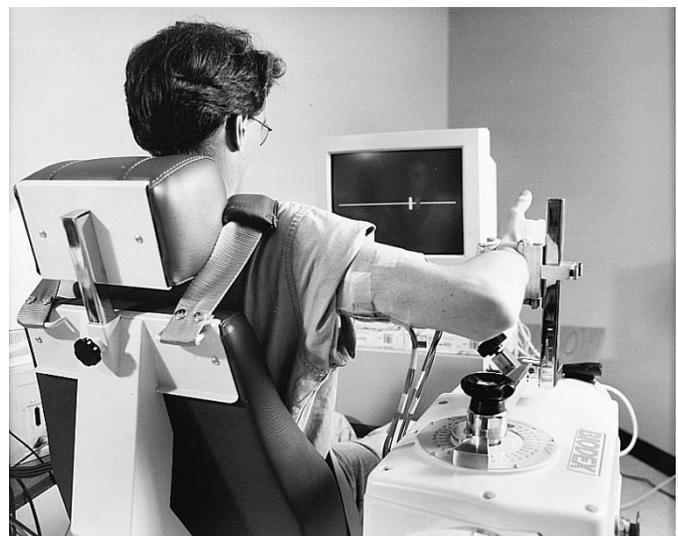


Fig. 2. Experimental apparatus as viewed from the rear. Subject is seated and secured in the exercise machine. Subject's right arm is rigidly cuffed to the dynamometer. Arrays of electrode-amplifiers are applied over the biceps and triceps muscles. The Target Tracking PC, situated directly in front of the subject, displays the EMG amplitude difference generated by the subject and the target.

tered about the muscle midline. The two contacts of each electrode-amplifier were oriented along the long axis of the arm (presumed direction of action potential conduction). The distance between adjacent electrode-amplifiers was approximately 1.75 cm. A single ground electrode was placed in the vicinity of the electrode-amplifiers. Each electrode-amplifier

had a pair of 4 mm diameter, stainless steel, hemispherical contacts separated by a distance of 15 mm (center to center). Each electrode-amplifier had a gain of 725, a common mode rejection ratio of approximately 90 dB at 60 Hz and a second-order 10–2000 Hz bandpass filter. Each EMG signal was electrically isolated, amplified and low-pass filtered. Amplification was achieved using the standard inverting gain operational amplifier configuration, with gain selectable from -1 to -25 for each EMG channel. The low-pass filter stage was unity gain, fourth-order with a cutoff frequency of 2000 Hz, achieved using a switched capacitor Butterworth low-pass filter (National Semiconductor model MF4-50, Santa Clara, CA). As a measure of total EMG system noise, data were recorded while subjects were asked to rest their arm completely. The resultant RMS signal level (representing equipment noise as well as ambient physiological activity recorded by the electrode-amplifiers) was on average $7.2 \pm 5.7\%$ of the RMS EMG at 50% MVC.

The EMG signals and the dynamometer signal were connected to a 16 channel 16-bit A/D converter (Computer Boards model CIO-DAS1600/16, Mansfield, MA) on an IBM-compatible PC. This “EMG Workstation PC” was outfitted with custom processing/display/data-logging software [33]. The EMG Workstation PC acquired the input data at a sampling rate of 4096 Hz per signal, formed a four-point moving average (all moving average coefficients set to 1.0) and decimated the data to 1024 Hz. The EMG Workstation PC then computed EMG amplitude estimates in real-time, formed the difference between the triceps and biceps amplitude, and sent the resulting differences out its serial port. The processing paradigm introduced a time delay of less than 8 ms in the EMG amplitude estimates. As a preprocessing step, individual channel offsets (representing offsets due to the A/D converter and front-end electronics) were subtracted from each signal. Four different EMG processors per muscle group (biceps/triceps) were then simultaneously produced from the offset-adjusted input EMG signals as follows.

1) Conventional single-channel MAV processing with a fixed smoothing window length of 250 ms, normalized to a 50% MVC. Note that an electrode-amplifier most central on the muscle was used.

2) and 3) Four-channel processors with fixed smoothing window lengths of 100 and 250 ms, respectively, were formed by equalizing the variance of each channel (based on calibration from a 50% MVC trial), followed by spatial-temporal MAV detection [26]. Note that spatial uncorrelation was not performed, since prior work [11] showed that it provided little performance improvement with this electrode arrangement.

4) A four-channel adaptive (first derivative), causal smoothing window length processor was formed by equalizing the variance of each channel (same calibration as processors 1–3), averaging the absolute values of the four channels, followed by adaptive window length MAV detection. The constant g was set to 547/s (see [26, Table II]). The duration of data contributing to the polynomial (Savitsky–Golay) differentiator was 375 ms (*the best duration for a 1 Hz target*). Adaptation of the smoothing window length was limited to a change of 0.5 samples (or ≈ 0.5 ms) per iteration.

For each experimental tracking trial, one triceps–biceps EMG amplitude *difference* was sent out the serial port (at a rate of 30 Hz) to a second “Target Tracking PC” which displayed the signal and a dynamic target to pursue. This PC had a 17 inch monitor situated at eye height, 2–3 feet in front of the subject. In Mode 1, the target moved horizontally on the screen as a band-limited (0.25 Hz) uniform random process. The range of the random process was scaled from 50% MVE flexion to 50% MVE extension. The horizontal center of the screen corresponded to no effort (0% MVE). The full width of the screen was scaled from 62.5% MVE flexion to 62.5% MVE extension in order to accommodate overshoot. Mode 2 used a similar target, except that the statistical bandwidth of the target was 1 Hz. In Mode 3, the target moved horizontally along the display in a random binary fashion, alternating between 25% MVE flexion and 25% MVE extension. The duration of time that the target remained at a particular level was random, selected as an independent uniform random variable over the range of 2–5 s. Although this target style was not studied in the simulation work, it tested the adaptive algorithm at its two extremes—rapid (step) changes combined with constant periods. The Target Tracking PC captured and stored sections of the input difference signal and the tracking target value to disk.

B. Experimental Methods

Informed consent was received from each subject. Nineteen subjects, 9 male and 10 female, ranging in age from 18 to 65 yr, each completed one experiment. Subjects had no known neuromuscular deficits of the right shoulder, arm or hand. The electrodes were applied and the subject was secured into the exercise machine. During an experimental trial, the subject was instructed to relax all muscles not directly involved in the task, and to maintain a consistent posture and contraction technique during and throughout all trials. Two two-second MVC trials (with a three minute rest after each trial) were conducted both for flexion and extension contraction. The average maximum dynamometer signal voltage provided a rough estimate of the dynamometer voltage corresponding to MVC. Using these contractions as a guide, the gain settings of each EMG channel were adjusted so that they would utilize as much of the resolution of the A/D board on the EMG Workstation PC as possible without saturating.

The subjects next performed five-second, constant-angle, constant-force contractions. The output voltage of the dynamometer and a static target signal level were simultaneously presented to the subject on the Target Tracking PC. The subject was instructed to begin at rest, then gradually (typically over a period of 0.5–1 s) increase flexion/extension torque until the target torque level was achieved. By observing the Target Tracking PC, the subject maintained the target torque level until a five-second segment of data was recorded. A rest period of two minutes was provided between trials. Two contractions each at 50% MVC flexion, 50% MVC extension and 0% MVC were recorded. A flexion contraction was used to calibrate EMG processors from flexion electrode channels, and an extension contraction was used to calibrate EMG processors from

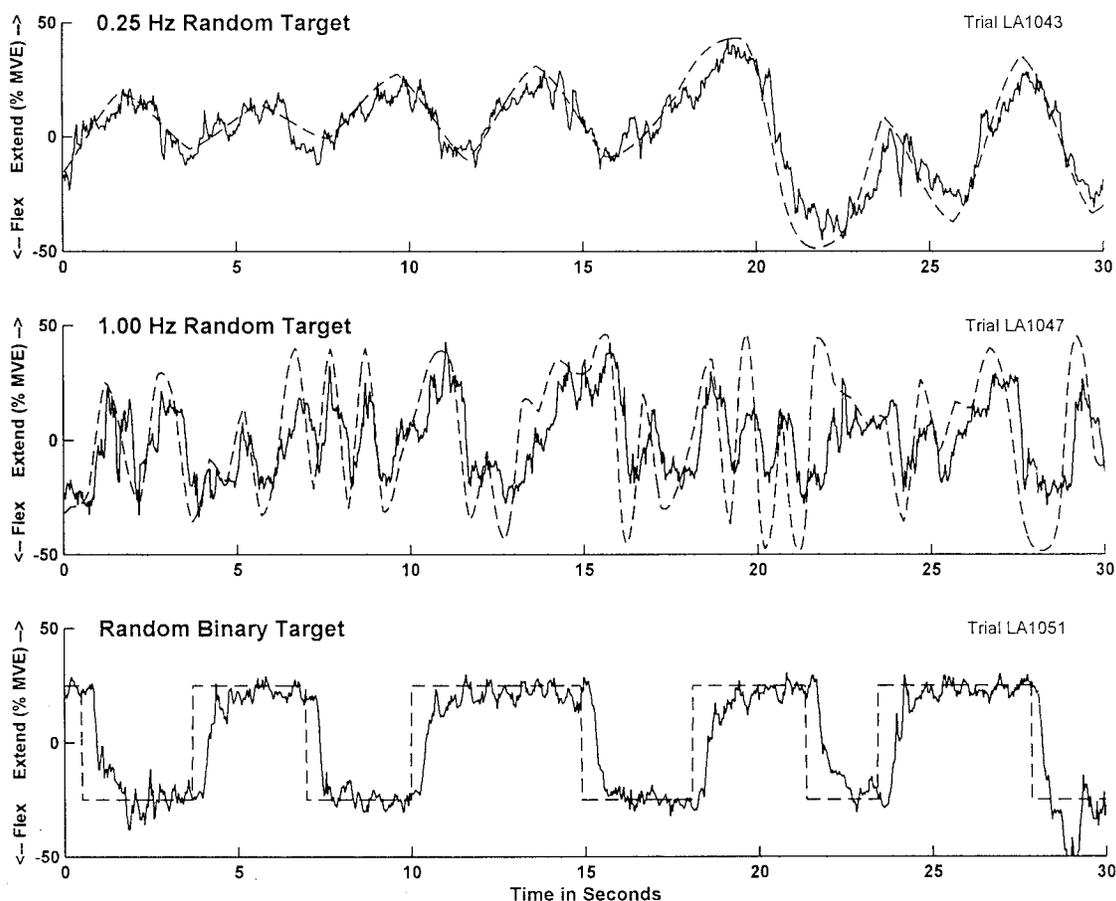


Fig. 3. Example data from tracking trials. Dash lines are the target, solid lines are the subject EMG amplitude pursuit profiles. Y-axis values give the EMG amplitude difference (scaled to percent MVE), with positive values denoting extension (i.e., triceps EMG amplitude greater than biceps EMG amplitude) and negative values denoting flexion. EMG processing was with the multiple-channel adaptive processor in each trial.

extension channels. These contractions were used to set the offset and equalize the variance of each EMG signal channel. Additionally, these contractions provided a reference (i.e., initial) calibration of the 50% MVE flexion/extension values. These MVE values were then adjusted to insure that subjects could reach the full extent of the target range. Adjustment was required for subjects displaying significant cocontraction on the 50% MVC trials, since reference calibration was based on either flexion or extension electrode channels while the target displayed their difference.

The subjects then performed a series of constant-angle, force-varying tracking task contractions. One triceps–biceps EMG difference and a dynamic target were simultaneously presented to the subject on the Target Tracking PC. The subject was blinded as to which EMG processor was selected. The subject was instructed to flex/extend about the elbow as necessary in order to produce an EMG difference signal which tracked the target as best as possible. This control strategy mimics the use of an EMG-controlled upper-limb prosthesis. After a transient warm-up period of a few seconds, 30 s of data were recorded. A series of three sets of tracking contractions was conducted. Each set randomly presented all 12 combinations of EMG processors (4) and tracking modes (3). A rest period of two minutes was provided between trials. After each set, 0% MVC data were also collected. Between

contractions the subject was released from the wrist cuff to prevent impaired blood flow to/from the hand.

C. Experimental Results

Fig. 3 shows sample tracking data for each of the three tracking tasks. Analysis of the tracking tasks consisted of evaluating the RMS error between the target and the subject's pursuit path. Statistical comparisons were made using the SAS software package, version 6 (SAS Institute Inc., Cary, NC). During the experiment it appeared that subjects were learning the tracking task during the first set of targets. This observation was confirmed statistically in that the tracking errors from the first tracking set were statistically different (larger) than those from the remaining two sets ($p \leq 0.02$ using a one-way ANOVA). For these reasons, data from the first tracking set were removed from further analysis. In addition, the data from one subject were excluded because the tracking errors were more than three standard deviations greater than the mean error. The remaining error results are presented in Table V.

Table V compares the single- versus multiple-channel, fixed-window, 250 ms detectors. Table V shows that the multiple-channel detector performed better than the single-channel detector for all target types ($p \leq 0.005$ for each target type using a t -test). The average error decreased 14.3% for the

TABLE V
MEAN \pm STANDARD DEVIATION TRACKING ERROR IN PERCENT MVE.
RESULTS IN EACH CELL ARE AVERAGED ACROSS 18 SUBJECTS

EMG Processor	Target Type		
	0.25 Hz Random	1.00 Hz Random	Random Binary
Single: Fixed, 250ms	8.67 \pm 2.34	21.51 \pm 3.07	17.91 \pm 1.51
Multiple: Fixed, 250ms	7.43 \pm 1.51	19.59 \pm 2.85	17.16 \pm 1.41
Multiple: Fixed, 100ms	9.43 \pm 2.14	19.69 \pm 2.85	16.94 \pm 1.51
Multiple: Adaptive	8.68 \pm 2.32	19.57 \pm 2.77	17.04 \pm 1.25

0.25 Hz random target, 8.9% for the 1 Hz random target and 4.2% for the random binary target. This result continues to reinforce the improvement found using multiple-channel EMG amplitude estimation [1], [2], [9], [11]–[13]. In practical applications, the advantages of this improvement must be weighed against the cost of the additional EMG channels.

For the 1 Hz random target, performance of the three multiple-channel algorithms was not statistically different ($p = 0.95$ using a one-way ANOVA). The simulation results suggested that the 100 ms fixed-window and adaptive processors should have performed equally well, but with 74% of the error of the 250 ms fixed-window processor. Perhaps the lack of differences was due to the task difficulty. Subjects noted that the 1 Hz bandwidth tracking task was a challenge. Thus, the errors may have been dominated by the difficulty subjects had tracking the target at this high bandwidth, with smaller errors related to processor performance not easily detected.

For the 0.25 Hz random target, the 250 ms fixed-window processor performed better than the 100 ms fixed-window processor ($p < 0.001$ using a t -test), as predicted by the simulations. No precise prediction was available for adaptive processing since the duration of data contributing to the polynomial derivative filter was not matched to this bandwidth (as it was in the case of the simulations). However, the experimental result fell between the two fixed-length detectors, as would be expected.

For the random binary target, performance of the three multiple-channel algorithms was not statistically different ($p = 0.67$ using a one-way ANOVA). Of interest with this tracking mode was to plot subject tracking performance as a function of the time from a binary level transition. Fig. 4 shows the average subject target tracking profiles, shown separately for transitions to 25% MVE extension and transitions to 25% MVE flexion. Since all transitions were followed by a minimum of 2 s before the next transition, only 2 s after a transition is shown. This figure shows that the error is dominated by subject delay in recognizing and reacting to the level change. Once a level change is initiated, the 100 ms multiple-channel fixed-window processor changes the fastest, closely followed by the adaptive processor. The adaptive processor might have changed even faster if the adaptation rate limit value had been set to a higher value. After the new level has been achieved, the 250 ms multiple-channel fixed-window processor and the adaptive processor seem to display the lowest average errors. Hence, the adaptive processor displays some of the better properties of each of the two fixed-length processors for this tracking mode. These observations are consistent with those found by Meek and Fetherston [19].

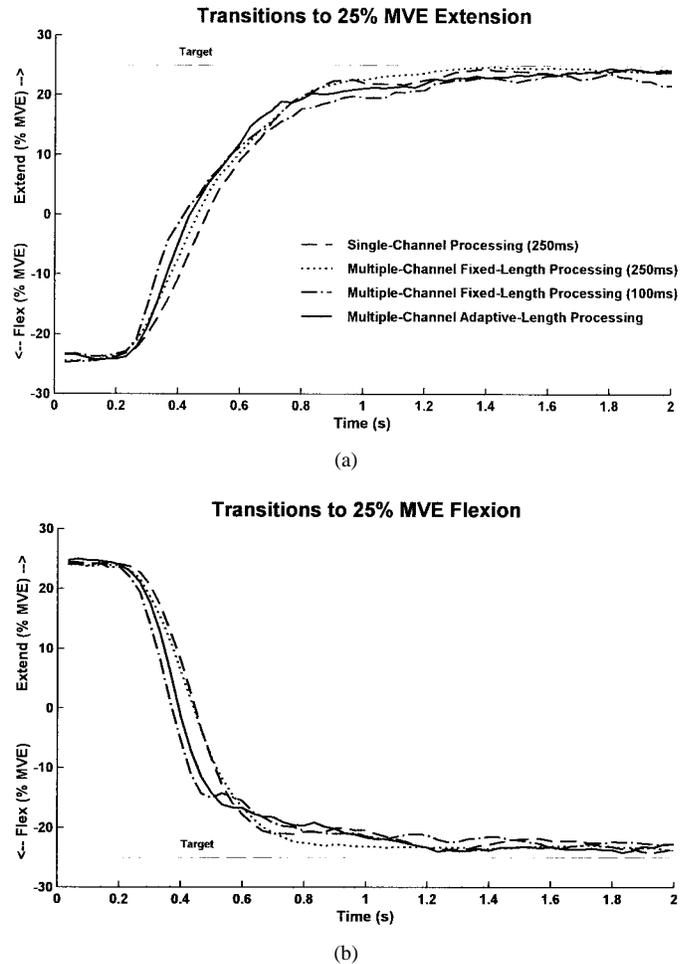


Fig. 4. Average target tracking responses for each EMG processor after a transition in random binary target tracking. Each graph line is the average of between 136 and 140 transitions. Top graphs show the first two seconds after the random binary target has transitioned from 25% MVE flexion to 25% MVE extension. Bottom graphs show the first two seconds after the random binary target has transitioned from 25% MVE extension to 25% MVE flexion. Y-axis values give the EMG amplitude difference, scaled to percent MVE.

V. DISCUSSION

A. Comparison of Theoretical Models to Prior Research

The theoretical modeling provided four optimum window length solutions, depending on the causality of the processing (causal versus noncausal) and the manner in which EMG amplitude was allowed to change in the local neighborhood of the sample index (quadratic versus linear). For two of these cases, causal linear and noncausal quadratic, an analytic solution to the optimum window length was available. A third case, the noncausal linear model, actually has no solution, so an approximate solution was coerced. The simulations demonstrated that the linear model was generally best for causal processing and the quadratic model was best for noncausal processing—the cases which have analytic solutions.

For the causal quadratic model, an analytic optimum window length was not available; thus, a numerical solution was used. D'Alessio [7], [18] developed a similar window length optimization model. He provided an approximate analytic solution to this problem by combining the results from

two limiting cases. The first limiting case is when the first derivative term is the dominant contributor to the error. In this case, D'Alessio set the second derivative to zero, essentially forming the causal linear model described in this paper. His analytic solution for that case matches that presented here. The second limiting case is when the second derivative term is the dominant contributor to the error, formed by setting the first derivative to zero. The complete solution was taken as the minimum window length specified by the two limiting cases. In addition, D'Alessio studied the noncausal processing problem. His quadratic solution does not match that of the current paper since it contains a first derivative term and a different power law relation (see [7, Eq. (11)]).

The causal linear solution for optimum window length (8), derived for discrete-time systems, is also nearly identical to the causal linear solution found by Park and Meek [20, Eq. (16)], which they derived for continuous-time systems. Their scaling factor was not derived analytically; rather numerical solution to the window length optimization problem was computed off-line for various values of the ratio and then the factor determined by least squares fit to the power law. The technique presented here determines the scaling factor analytically, allowing direct extension of adaptive window length selection to noncausal processing, multiple EMG channels and white versus nonwhite processing.

B. Discussion of Simulation and Experimental Studies

Both this simulation study and that of D'Alessio [7] found a strong dependence in adaptive processor performance on the quality of the EMG amplitude derivatives. Note that the simulation work of D'Alessio evaluated the EMG amplitude while it varied as a sine wave. When the derivative estimates degraded, adaptive processor performance degraded. Both studies also found that the length of data contributing to the derivative estimate should decrease as the EMG amplitude bandwidth (for the random tracking trials studied here) or frequency (for the sinusoidal trials studied by D'Alessio) increased. If the best derivative technique was tuned to the target bandwidth/frequency, then the adaptive algorithm performed approximately as well as the best fixed-length processor. Unfortunately, this result means that the burden of selecting the optimum window length in the fixed-length case is replaced by the burden of selecting the best derivative filter in the adaptive-length case. Future research should be directed toward improved derivative filters that do not require operator tuning to the signal bandwidth. If automated high quality differentiation can be accomplished, then the simulation results suggest that adaptive window length processing can select the best possible window length for all bandwidths of these random changes in EMG amplitude, and perhaps in general. Note that even if better derivative algorithms are not found, the random binary mode studied in this experiment demonstrated how the step response of the adaptive processor could simultaneously mimic the rapid response of a short-duration window during the level transition and the low variance of a long duration window during the plateau. For certain applications, e.g., control of an upper-

limb prosthesis, this characteristic may be quite attractive. In addition, Park and Meek [20] have demonstrated situations in which adaptive processing, using a derivative filter which is not tuned to the signal bandwidth, exhibits performance superior to certain fixed-length processors. Finally, it may prove more accurate to directly estimate the ratio of the EMG amplitude divided by its applicable derivative, rather than separately estimating the numerator and denominator terms in the optimal window length formulae.

In contrast to the work of D'Alessio [7], these simulations suggest that second derivatives of EMG amplitude can be used effectively for noncausal amplitude estimates. This result has yet to be evaluated with experimental data. The simulation studies also found that the performance of the adaptive algorithm was not sensitive to the rate at which adaptation was allowed to take place. Extremely slow adaptation gave performance results identical to rapid adaptation. This result seems to be due to the fact that the best adaptive algorithm performed about as well as the best fixed-length processor. When the adaptation was set to its slowest rate, the adaptive window length seemed to migrate to a relatively static value. This value was equal to the best fixed-length window which gave performance similar to when adaptation was rapid. It is not clear if this result can be directly extrapolated to situations other than the band-limited uniform random target tracking studied here. In the experimental study, the adaptive window length was allowed to change by 0.5 samples per iteration.

All of the experimental errors listed in Table V are considerably larger than the simulation errors listed in Tables III and IV. This result is expected for at least two reasons. First, the simulation errors do not account for the imprecise ability of subjects to track the target. This error grows with the difficulty (bandwidth) of the target being tracked [34]. Second, the simulations evaluated estimation errors from a single EMG amplitude estimate, but the experiment evaluated errors which were formed from the difference of two EMG amplitude signals. The random error of this difference signal should be greater. (If the errors in the individual signals were uncorrelated, their variances would sum.)

Note that, as with much of the prior work done in this field, all of these results are influenced by the choice of minimum MSE as the optimization criterion. For certain applications (e.g., multistate function selection in prosthetic control), future research may wish to develop an adaptive window length EMG processor which provides the lowest maximum displacement between the output of the estimator and the true EMG amplitude. For this application, minimizing the maximum error may be more effective in reducing selection errors than would occur using minimum MSE.

VI. SUMMARY AND CONCLUSIONS

A technique for adaptive window length estimation of the amplitude of the dynamic EMG signal was derived. This method includes consideration of the first and second derivative of the EMG amplitude. Simulation and experimental studies investigated the ideal and practical performance of

the technique in comparison to fixed-length processors, when the EMG amplitude was changing as a band-limited, uniform random process. These studies found the advantages of the adaptive processor to be situation dependent. In the simulation study, practical adaptive detectors, with optimum selection of a polynomial derivative filter, worked as well as the optimum fixed-length processor. For such situations, a fixed-length detector is likely preferred, because the distribution of error between bias and variance is more stable. Future research should be directed toward improved derivative filters which may alter this conclusion.

Experimentally, it was confirmed that multiple-channel processors performed better than the single-channel processor. Perhaps due to task difficulty, no differences in the multiple-channel processors were observed at the 1 Hz target bandwidth. Results at the 0.25 Hz bandwidth were consistent with simulation predictions. With the random binary target, the adaptive processor displayed a rapid response during level transitions and low variance when the EMG amplitude target was constant. These results suggest that when the EMG amplitude varies as a band-limited uniform signal of known, fixed bandwidth (or in a sine wave fashion, of known, fixed frequency [7], [18]), then adaptive window length processing does not provide an advantage over fixed-length processing. In other situations (e.g., when EMG amplitude changes in a random binary fashion or when the processor is not allowed to tune its derivative filter length and fixed window smoothing length to the signal bandwidth/frequency), adaptive window length processing may be advantageous.

APPENDIX

TWO EXTENSIONS TO THE THEORETICAL MODELS

First, the above modeling assigned equal weighting to the squared bias error and the variance error in the MSE minimization. There may be circumstances in which a different relative weighting is desired. A simple method for doing so is to introduce a multiplicative weighting constant w to the variance error in (1) (e.g., $w = 2$ will double the importance of variance error). For the noncausal quadratic window formula shown in (8), the weighting results in replacing the term 72 with the term $72 \cdot w$. Similarly for the causal linear formula shown in (9), the weighting results in replacing the term f with the term $f \cdot w^{1/3}$. Note that the resultant theoretical MSE will be weighted.

Second, in some situations an optimal fixed window length is desired. To select this window length, choose the fixed window length N which minimizes the average MSE over all available samples. Thus, pick the N that minimizes $Error = (1/T) \sum_{t=1}^T MSE(t)$, where the range of available samples is from 1 to T . If (1) is substituted into this equation, then mathematical steps identical to those given previously result, except that the sample-dependent terms $s^2(t)$, $\dot{s}^2(t)$ and $\ddot{s}^2(t)$ are replaced with their sample averages $s_{AVE}^2 = (1/T) \sum_{t=1}^T s^2(t)$, \dot{s}_{AVE}^2 and \ddot{s}_{AVE}^2 . Thus, the optimal fixed window length can be determined from the average value of the square of EMG amplitude and its derivatives.

ACKNOWLEDGMENT

The author is grateful for the comments, critique, and technical support provided to the project by K. Farry, G. Hampel, S. Martin, S. Meek, T. Murphy, L. Simmons, M. Smits, and P. Teare.

REFERENCES

- [1] N. Hogan and R. W. Mann, "Myoelectric signal processing: Optimal estimation applied to electromyography—Part I: Derivation of the optimal myoprocessor," *IEEE Trans. Biomed. Eng.*, vol. BME-27, pp. 382–395, July 1980.
- [2] ———, "Myoelectric signal processing: Optimal estimation applied to electromyography—Part II: Experimental demonstration of optimal myoprocessor performance," *IEEE Trans. Biomed. Eng.*, vol. BME-27, pp. 396–410, July 1980.
- [3] V. T. Inman, H. J. Ralston, J. B. de C. M. Saunders, B. Feinstein, and E. W. Wright, "Relation of human electromyogram to muscular tension," *EEG Clin. Neurophysiol.*, vol. 4, pp. 187–194, 1952.
- [4] J. G. Kreifeldt, "Signal versus noise characteristics of filtered EMG used as a control source," *IEEE Trans. Biomed. Eng.*, vol. BME-18, pp. 16–22, Jan. 1971.
- [5] J. G. Kreifeldt and S. Yao, "A signal-to-noise investigation of nonlinear electromyographic processors," *IEEE Trans. Biomed. Eng.*, vol. BME-21, pp. 298–308, Apr. 1974.
- [6] E. A. Clancy and N. Hogan, "Single site electromyograph amplitude estimation," *IEEE Trans. Biomed. Eng.*, vol. 41, pp. 159–167, Feb. 1994.
- [7] T. D'Alessio, "Some results on the optimization of a digital processor for surface EMG signals," *Electromyogr. Clin. Neurophysiol.*, vol. 24, pp. 625–643, 1984.
- [8] G. C. Filligoi and P. Mandarini, "Some theoretic results on a digital EMG signal processor," *IEEE Trans. Biomed. Eng.*, vol. BME-31, pp. 333–341, Apr. 1984.
- [9] M. I. A. Harba and P. A. Lynn, "Optimizing the acquisition and processing of surface electromyographic signals," *J. Biomed. Eng.*, vol. 3, pp. 100–106, 1981.
- [10] E. Kaiser and I. Petersen, "Adaptive filter for EMG control signals," in *The Control of Upper-Extremity Prostheses and Orthoses*, P. Herberts, R. Kadefors, R. Magnusson, and I. Peterson, Eds. Springfield, IL: Charles C. Thomas, 1974, pp. 54–57.
- [11] E. A. Clancy and N. Hogan, "Multiple site electromyograph amplitude estimation," *IEEE Trans. Biomed. Eng.*, vol. 42, pp. 203–211, Feb. 1995.
- [12] W. R. Murray and W. D. Rolph, "An optimal real-time digital processor for the electric activity of muscle," *Med. Instrum.*, vol. 19, pp. 77–82, 1985.
- [13] S. Thusneyapan and G. I. Zahalak, "A practical electrode-array myoprocessor for surface electromyography," *IEEE Trans. Biomed. Eng.*, vol. 36, pp. 295–299, Feb. 1989.
- [14] C. Hershler and M. Milner, "An optimality criterion for processing electromyographic (EMG) signals relating to human locomotion," *IEEE Trans. Biomed. Eng.*, vol. BME-25, pp. 413–420, May 1978.
- [15] H. Miyano, T. Masuda, and T. Sadoyama, "A note on the time constant in low-pass filtering of rectified surface EMG," *IEEE Trans. Biomed. Eng.*, vol. BME-27, pp. 274–278, May 1980.
- [16] F. Q. Xiong and E. Shweddyk, "Some aspects of nonstationary myoelectric signal processing," *IEEE Trans. Biomed. Eng.*, vol. BME-34, pp. 166–172, Feb. 1987.
- [17] R. B. Jerard, T. W. Williams, and C. W. Ohlenbusch, "Practical design of an EMG controlled above elbow prosthesis," in *Proc. 1974 Conf. Eng. Devices in Rehabilitation*, Boston, MA, 1974, pp. 73–77.
- [18] T. D'Alessio, "Analysis of a digital EMG signal processor in dynamic conditions," *IEEE Trans. Biomed. Eng.*, vol. BME-32, pp. 78–82, Jan. 1985.
- [19] S. G. Meek and S. J. Fetherston, "Comparison of signal-to-noise ratio of myoelectric filters for prosthesis control," *J. Rehab. Res. Dev.*, vol. 29, pp. 9–20, 1992.
- [20] E. Park and S. G. Meek, "Adaptive filter of the electromyographic signal for prosthetic control and force estimation," *IEEE Trans. Biomed. Eng.*, vol. 42, pp. 1048–1052, Oct. 1995.
- [21] R. R. Fullmer, S. G. Meek, and S. C. Jacobsen, "Optimization of an adaptive myoelectric filter," in *Proc. Annu. Int. Conf. IEEE Eng. in Med. and Biol. Soc.*, 1984, pp. 586–591.
- [22] S. C. Jacobsen, S. G. Meek, and R. R. Fullmer, "An adaptive myoelectric filter," in *Proc. Annu. Int. Conf. IEEE Eng. in Med. and Biol. Soc.*, 1984, pp. 592–596.

- [23] S. Jacobsen, D. F. Knutti, R. T. Johnson, and H. H. Sears, "Development of the Utah artificial arm," *IEEE Trans. Biomed. Eng.*, vol. BME-29, pp. 249–269, Apr. 1982.
- [24] H. B. Evans, P. Zushan, P. A. Parker, and R. N. Scott, "Signal processing for proportional myoelectric control," *IEEE Trans. Biomed. Eng.*, vol. BME-31, pp. 207–211, Feb. 1984.
- [25] E. A. Clancy, "EMG amplitude estimation with adaptive smoothing window length," in *Proc. Annu. Int. Conf. IEEE Eng. in Med. and Biol. Soc.*, 1997, vol. 19, pp. 1271–1274.
- [26] Y. St-Amant, D. Rancourt, and E. A. Clancy, "Influence of smoothing window length on electromyogram amplitude estimates," *IEEE Trans. Biomed. Eng.*, vol. 45, pp. 795–800, June 1998.
- [27] J. S. Bendat and A. G. Piersol, *Random Data: Analysis and Measurement Procedures*. New York: Wiley, 1971.
- [28] W. H. Press, S. A. Teukolsky, W. T. Vetterling, and B. P. Flannery, *Numerical Recipes in C: The Art of Scientific Computing*, 2nd ed. New York: Cambridge Univ. Press, 1994, pp. 186–189, 650–655.
- [29] I. S. Gradshteyn and I. M. Ryzhik, *Table of Integrals, Series and Products*. New York: Academic, 1980, p. 1.
- [30] M. Bilodeau, M. Cincera, A. B. Arsenault, and D. Gravel, "Normality and stationarity of EMG signals of elbow flexor muscles during ramp and step isometric contractions," *J. Electromyogr. Kinesiol.*, vol. 7, pp. 87–96, 1997.
- [31] E. A. Clancy and N. Hogan, "Probability density of the surface electromyogram and its relation to amplitude detectors," this issue, pp. 730–739.
- [32] G. Giakas and V. Baltzopoulos, "Optimal digital filter requires a different cut-off frequency strategy for the determination of the higher derivatives," *J. Biomech.*, vol. 30, pp. 851–855, 1997.
- [33] E. A. Clancy, "A PC-based workstation for real-time acquisition, processing and display of electromyogram signals," *Biomed. Instrum. Tech.*, vol. 32, no. 2, pp. 123–134, 1998.
- [34] K. R. Boff and J. E. Lincoln, Eds., *Engineering Data Compendium: Human Perception and Performance*. Wright-Patterson AFB, OH: AAMRL, 1988, pp. 1972–1973.



Edward (Ted) A. Clancy (S'83–M'91–SM'98) received the B.S. degree from Worcester Polytechnic Institute, Worcester, MA, and the S.M. and Ph.D. degrees from the Massachusetts Institute of Technology, Cambridge, MA, all in electrical engineering.

He has worked in industry as a research scientist for medical instrumentation companies with products in the areas of EEG, ECG and blood pressure analysis. He is a Researcher at the Liberty Mutual Research Center for Safety and Health in Hopkinton, MA, and holds the appointment of Professeur

Associé at Laval University, Québec, Canada. His research interests are in signal processing, stochastic estimation, and system identification, particularly as applied to problems in medical engineering and human rehabilitation.